UCID-19369

SCOPING ANALYSIS FOR RADIONUCLIDE MIGRATION TEST

Frank A. Morrison, Jr.

January 1982

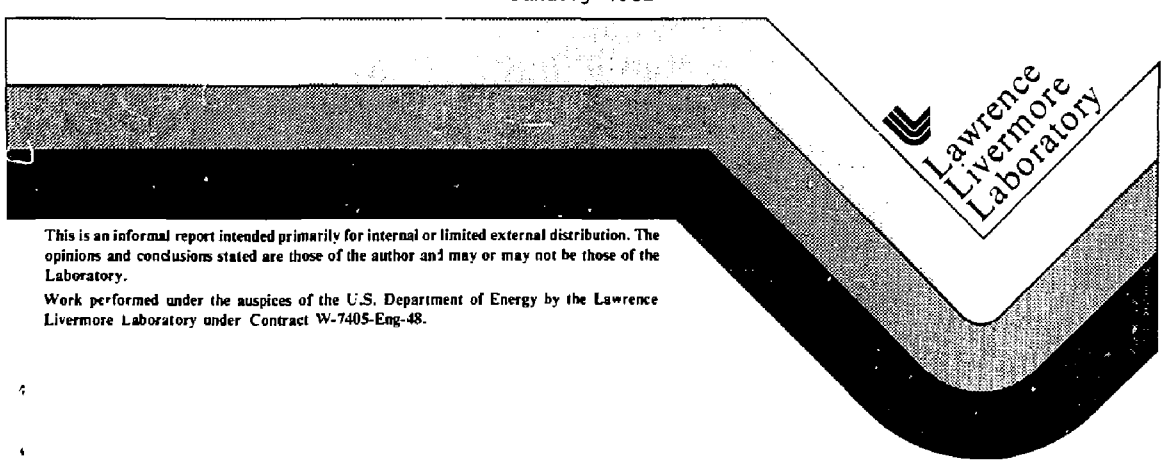

UCID--19369

DE82 014893

ABSTRACT

The Lawrence Livermore National Laboratory is to conduct an *in situ* test of radionuclide migration in fractured granite. Radionuclides are to be injected into a fracture in the Climax Stock of the Nevada Test Site, then transported by fluid motion and subsequently withdrawn. The fluid will be injected through a borehole intersecting a near vertical fracture and withdrawn through a second borehole that intersects the fracture directly below the first.

The scoping calculations presented here are intended to aid planning this experiment. In the absence of a detailed fracture description, this analysis treats the fracture as the space between parallel flat plates; the flow is a Hele-Shaw flow. The calculations predict the conditions for breakthrough of radionuclides at the outlet hole and describe the subsequent concentration history of fluid flowing from the fracture. The effects of advection, sorption and geometric dispersion are treated.

FLOW IN A FRACTURE

Saturated creeping flow in the gap between two parallel plates is called plane Poiseuille flow. The fluid flows through the fracture, while adhering to the bounding surfaces, in response to pressure gradients and gravity. Averaging this velocity across the gap yields a mean velocity u varying as the square of h, the gap thickness.

$$u = -\frac{h^2}{12\mu}(\nabla p + \rho g z) \qquad (1)$$

Here, μ is the fluid viscosity, p the pressure, ρ the fluid density, g the acceleration of gravity and z an upward directed unit vector. The flow is a potential flow. For simplicity, we define the pressure

$$P = p + \rho g z \qquad (2)$$

analogous to the piezometric head. In gravitational equilibrium, P is uniform.

Continuity of fluid flow, together with the expression for average velocity combine to yield

$$\nabla^2 P = 0 \qquad (3)$$

This well known result, that the flow is governed by Laplace's equation, allows us to readily use results obtained in several other fields of physics.

FLOW BETWEEN BOREHOLES: NO SUPERPOSED FLOW

In a few circumstances, the effect of gravity is either negligible or readily incorporated into the analysis. In a horizontal fracture, gravity acts normal to the flow and does not affect fluid motion. If the velocities produced by injection into a vertical fracture greatly exceed the gravitational flow, the effect of gravity may be neglected. Finally, if the fluid far from injection is in hydrostatic equilibrium, the analysis follows that of tne horizontal fracture, with P replacing p. These cases are distinguished from the case later treated, that of a fracture with a uniform flow superposed on the induced flow between boreholes, and are treated in this section.

Consider injection into an unbounded homogeneous fracture from one borehole, coupled with extraction from the second hole at the same volume flow rate, $\dot{V}$. This corresponds to the well known potential distribution corresponding to a source and sink of equal strength. This distribution has been used in hydrologic application to describe two well tracer tests in aquifers [1]

The streamlines and lines of constant pressure are coordinates of a bipolar coordinate system. Moon and Spencer [2] describe this coordinate

system in detail. P is constant on non-concentric circles about the boreholes. Streamlines, ψ, are circular arcs connecting the boreholes. The flow is shown in Figure 1. A more general analysis with unequal rates at the two holes could readily be performed. Some streamlines would, in that case, remain open; they would not terminate at both boreholes.

The flow outside the boreholes is identical to that produced by a point source and point sink. These singularities are also shown in Figure 1. They are not precisely in the borehole centers, but for widely spaced boreholes as envisioned here, the difference is negligible. The distance, 2a, between source and sink is, for all practical purposes, the distance between borehole centers.

The solution for the stream function is readily found to be

$$\psi = \frac{\dot{V}}{2\pi h} \tan^{-1} \frac{-2ay}{x^2 + y^2 - a^2} \qquad (4)$$

corresponding to the circular arcs described above. Fluid, injected into the fracture, will flow to the extraction borehole on any of these streamlines. The time to traverse between boreholes will, however, depend strongly on the streamline travelled. The longer streamlines are also those with lower fluid velocity.

Tracers or radionuclides injected at one borehole and moving on different streamlines will arrive at the other borehole at different times, resulting in an apparent or 'geometric' dispersion. The effect is present in a purely advective transport; any molecular dispersion would be superposed.

The time for fluid to travel along any streamline is

$$t = \int_{\psi} \frac{ds}{u} \qquad (5)$$

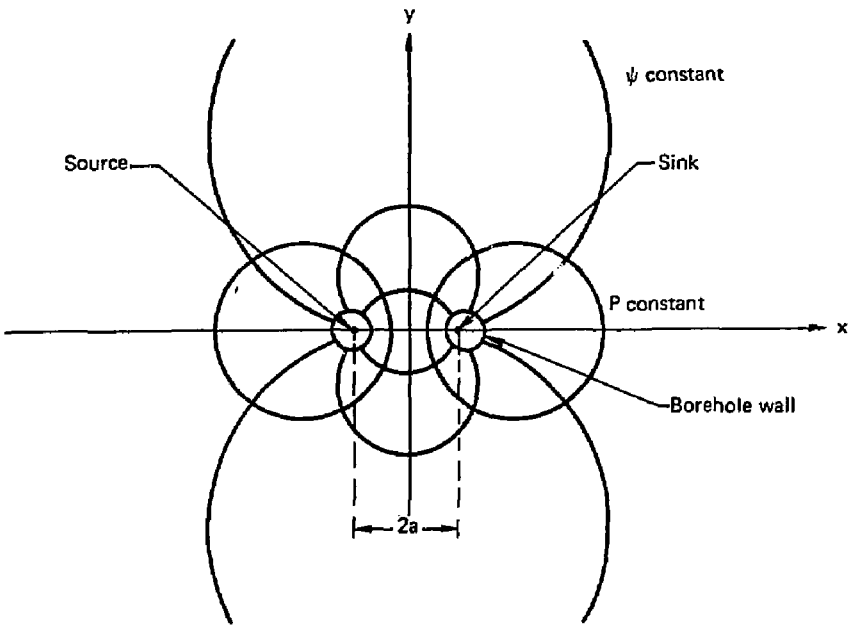

Figure 1. Flow resulting from a source and sink has nonconcentric circular streamlines.

where the integration is along the streamline. The time to travel between boreholes is, aside from the comparitively short times to travel between the singularities and the borehole walls, equal to the time to travel between source and sink.

Calculation of transit times appears to be a peculiarly hydrologic pursuit. Thus, while analogies to eq. (4) abound in the literature, Grove and Beetem [1] first calculated this time for the distribution given in eq. (4). As their analysis is somewhat more complicated than necessary, we offer an alternative derivation that provides insight into the flow.

First, using eq. (4), we can demonstrate that the fluid speed at any point depends only on the distances from the two boreholes.

$$u = \frac{\dot{V}a}{\pi h r_1 r_2} \tag{6}$$

where r_1 and r_2 are the distances to the source and sink. See Fig. 2. Figure 2 also defines angles α and γ which are employed in the calculation. R_o is the radius of curvature of the circular arc ψ.

$$R_o = a/\sin\gamma \tag{7}$$

and

$$\gamma = 2\pi h\psi/\dot{V} \tag{8}$$

Using the angles shown in Fig. 2, we readily write eq. (6) as

$$u = \frac{\dot{V}a}{4\pi h R_o^2 \sin\frac{\alpha}{2}\sin(\gamma - \frac{\alpha}{2})} \tag{9}$$

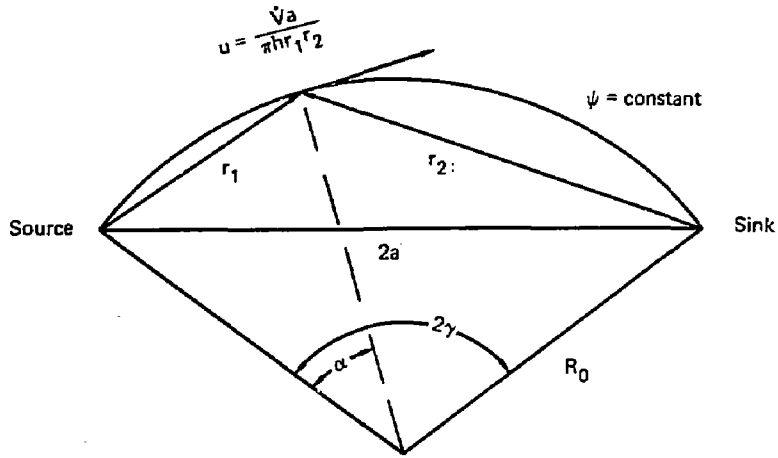

Figure 2. Flow along a streamline arc is readily described in geometric terms.

ine integral (5) then is

$$t = \int_0^{2\gamma} \frac{R_o \, d\alpha}{u} \tag{10}$$

with u given by eq. (9). The expression integrates immediately to yield

$$t = \frac{4\pi h a^2}{\dot{V}} \quad \frac{\sin\left(\frac{2\pi h \psi}{\dot{V}}\right) - \frac{2\pi h \psi}{\dot{V}} \cos\left(\frac{2\pi h \psi}{\dot{V}}\right)}{\sin^3\left(\frac{2\pi h \psi}{\dot{V}}\right)} \tag{11}$$

The shortest path is, of course, the straight line connecting the singular points, ψ equal to zero. One readily verifies that, along this streamline,

$$t = \frac{4\pi h a^2}{3\dot{V}} \tag{12}$$

or equivalently that a tracer moving will the fluid with reach the sink when a volume

$$V = \frac{4\pi h a^2}{3} \tag{13}$$

is injected. Without extraction, three times as much volume would need be injected for tagged fluid to reach the sink location.

As an example, 42 cc of fluid would be injected into a 10 μ fracture before a tracer moving with the fluid appears at an extraction borehole, 2 metres distant.

At any time, τ, greater than $4\pi h a^2/3\dot{V}$, some fraction, f, of the fluid arriving at the withdrawal borehole will have originated at the injection hole. This fraction can be expressed in terms of the stream function of the streamline whose transit time is τ.

$$f = \frac{2\psi(\tau)h}{V} \tag{14}$$

where $\psi(\tau)$ is found from eq. (11).

Consider, now, a chemical tracer, nonadsorbing and nondispersed, moving with this incompressible flow. The tracer, together with the fluid, is injected completely around the periphery of the injection hole. If the entering concentration everywhere is c_o and if the volume average concentration arriving at the second hole is, at any instant, c, then our fraction f is also

$$f = \frac{c}{c_o} \tag{15}$$

It is important to note that this is the concentration ratio for the fluid arriving at that instant. It is not the concentration in the fluid allowed to accumulate in the borehole. Combining eqs. (11), (13), and (15), we produce a relation between the volume injected and the average arriving concentration.

$$\frac{V_{injected}}{4\pi ha^2} = \frac{\sin\left(\pi \frac{c}{c_o}\right) - \frac{\pi c}{c_o}\cos\left(\pi \frac{c}{c_o}\right)}{\sin^3\left(\pi \frac{c}{c_o}\right)} \tag{16}$$

Eq. (16) is shown in Fig. 3. As fluid is injected, there is a finite period when no tracer appears at the second hole. Then, when tracer on the shortest path arrives, as given by eq. (13), the concentration begins to increase. The increase is rapid as fluid in adjacent envelopes arrives shortly thereafter. Subsequent increases in concentration are much slower and the asymptotic approach to a concentration ratio of unity is quite slow. The effect shown in Fig. 3 is due to geometric dispersion, an apparent dispersion resulting from the unequal transit times on different paths.

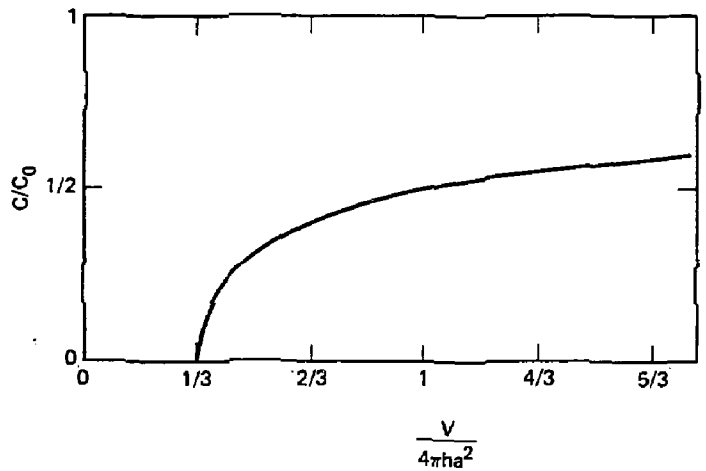

Figure 3. The concentration in the fluid arriving at the withdrawal borehole increases abruptly

Consider again the example of a 20 μ fracture with boreholes separated by 2 metres (a = 1 metre). As before, V is 42 cc at breakthrough. For the concentration ratio to reach 1/3, 65 cc must be injected. A total of 126 cc injected are required to produce a concentration ratio of 1/2.

An adsorbing species with a linear adsorbtion isotherm moves at an apparent speed

$$U_a = u/R \tag{17}$$

where R is a retardation factor greater than one. See Bear [3], for example. Travel times for this species are all R times as long as those of species traveling with the fluid. Breakthrough and concentration buildup are delayed proportionately. In our previous example, 420 cc would need to be injected prior to breakthrough of a species possessing a retardation factor of 10.

In the migration test, a finite volume of radionuclide solution will be injected. Water without radionuclides will then be injected as a pusher. While Fig. 3 and eq. (16) address continuous injection, they may be used in a straightforward way for finite volume injection. Any finite injection can be considered as a sum of continuous injections. Figure 4 shows schematically how a finite injection results from positive and negative continuous injections suitably spaced. The observed outlet concentration results from the corresponding sums obtained from Fig. 3. The concept can be immediately extended to describe any input variation.

Using Fig. 4 as a guide, we can extend the example that we have been developing. Suppose now that 100 cc of radionuclide solution is injected into the 10 μ fracture. Water, without radionuclides, is then injected to push the solution through. Withdrawal is 2 metres distant. When 42 cc of solution are injected, nonabsorbing species (R=1) break through. The concentration

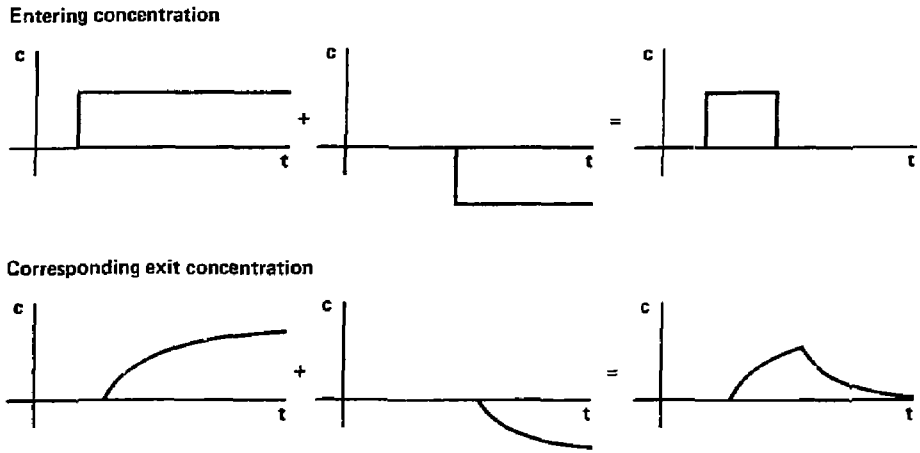

Figure 4. A finite injection is treated as a superposition of infinite injections.

entering the second borehole continues to rise until 142 cc has been injected; that is, 100 cc of solution followed by 42 cc of water. At this point, the concentration reaches its maximum. $V/4\pi ha^2$ is 1.13 and the concentration ratio is 0.52. Water breakthrough occurs at this point and the concentration subsequently drops rapidly.

Another species in the same injection has (say) a retardation factor of 10. When 420 cc (42*10) are injected, this species appears at the second borehole. When 100 cc of solution and 420 cc of water, a total of 520 cc, are injected, the trailing front breaks through. Concentration again is at a maximum. Now, however, $V/4\ \pi\ ha^2R$ is only 0.41 so the maximum concentration ratio is only 0.22.

FLOW BETWEEN BOREHOLES: UNIFORM FLOW SUPERPOSED

Now, we will extend consideration to flow with a superposed uniform flow. Such a flow could result from gravity. The radionuclide migration test will be performed in an unsaturated fracture. Prior to radionuclide injection, water could be injected at a high rate in an attempt to saturate the fracture. Then, with radionuclide injection occurring more slowly, this previously injected water would flow down under the influence of gravity, approximating a uniformly flowing sheet.

The flow with source, sink and a parallel stream is also a classical potential flow. The stream function is the superposition of the parallel flow stream function, Uy, and the stream function of eq. (4).

$$\psi = \frac{\dot{V}}{2\pi h} \tan^{-1} \frac{-2ay}{x^2 + y^2 - a^2} + Uy \qquad (18)$$

U is the speed of the parallel stream flowing in the x direction. Fluid, flowing freely (p constant) down a vertical fracture has, according to eq. (1), a speed given by

$$U = \frac{h^2 \rho g}{12\mu} \tag{19}$$

In a 10 μ vertical fracture, eq. (19) gives U for water about $8 * 10^{-5}$ m/s. The streamlines connecting the boreholes are, in this case, entirely contained within an oval bounding streamline. See Fig. 5. This oval is a Rankine oval, so named after W.J.M. Rankine who investigated these shapes and the potential flow about them [4]. More recently, Nelson [5] examined groundwater flow in such configurations. The equation of the bounding streamline is simply eq. (18) with ψ set equal to zero. Using this relation allows one to readily show that the length, X, of the bounding oval is

$$X = 2a\left(1 + \frac{\dot{V}}{\pi h a U}\right) \tag{20}$$

while the width Y is implicitly given by

$$\frac{Y}{4a} - \frac{a}{Y} = \cot\frac{\pi h Y U}{\dot{V}} \tag{21}$$

The relation was solved to find the width as a function of dimensionless flow rate. Both dimensions are shown in Figure 6. The dimensions of the bounding oval are significant because, in this ideal fracture, all the radionuclides remain within the oval.

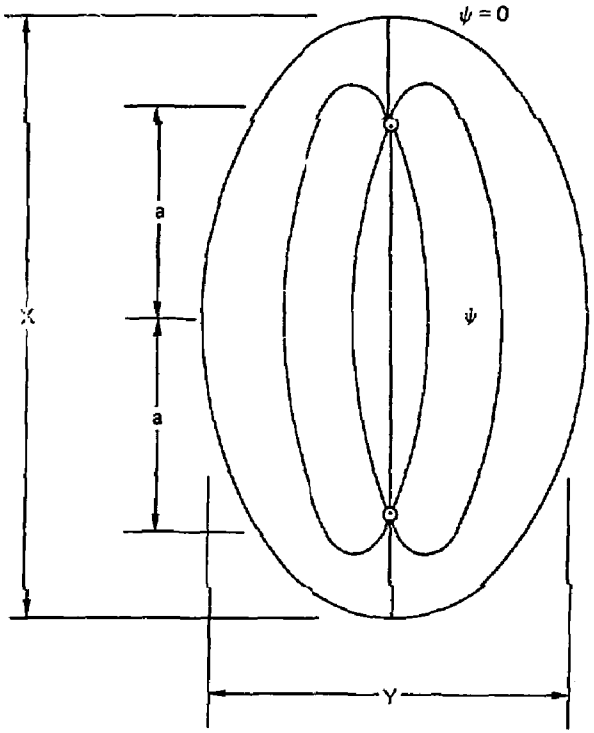

Figure 5. Flow between the boreholes remains within the bounding oval

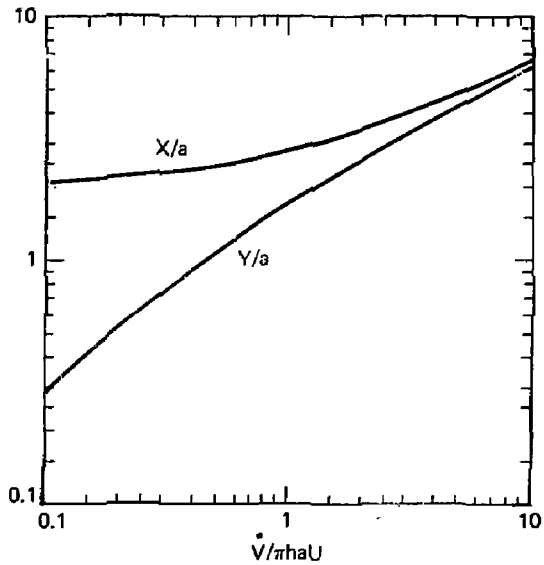

Figure 6. Dimensions of the bounding oval bound radionuclide transport

An example will illustrate the use of the figure. Consider an injection rate, $\dot{V}$, of 0.15 cc/min ($2.5 * 10^{-9}$ m^3/s) into a 10 μ fracture with U, as before, equal to $8 * 10^{-5}$ m/s and a equal to 1 m. The dimensionless injection rate is nearly 1.0. From Fig. 6, Y/a is 1.7 so the width of bounding oval is only 1.7a or 1.7m. X/a is about 2.8 so the length of the oval is 2.8 m.

We now examine this flow and the transit time distribution to find results analogous to those of the last section. Breakthrough times (or volumes) and concentration histories are needed, now as a function of the dominance of gravity.

Corresponding to the stream function (18) is the complex potential

$$\Omega = \frac{\dot{V}}{2\pi h} \ln \frac{z+a}{z-a} + Uz \tag{22}$$

The stream function is the imaginary part of this complex potential. The complex velocity is

$$w = \frac{d\Omega}{dz} = U - \frac{\dot{V}a}{\pi h(z^2 - a^2)} \tag{23}$$

As before, the fastest trip between boreholes is along the straight line connecting them. Using eq. (23) to evaluate the time,

$$t = \int_{-a}^{a} \frac{dx}{u} \tag{24}$$

The real component of w is the x component of velocity. Along this streamline, there is, of course, no y component.

$$t = \int_{-a}^{a} \frac{dx}{U - \frac{\dot{V}a}{\pi h(x^2 - a^2)}} \tag{25}$$

Integrating gives us, in contrast to eq. (12).

$$t = \frac{2a}{U}\left[1 - \frac{\frac{\dot{V}}{\pi haU}}{\left(1+\frac{\dot{V}}{\pi haU}\right)^{\frac{1}{2}}}\operatorname{ctnh}^{-1}\left(1+\frac{\dot{V}}{\pi haU}\right)^{\frac{1}{2}}\right] \tag{26}$$

or

$$V = \frac{2\dot{V}a}{U}\left[1 - \frac{\frac{\dot{V}}{\pi haU}}{\left(1+\frac{\dot{V}}{\pi haU}\right)^{\frac{1}{2}}}\operatorname{ctnh}^{-1}\left(1+\frac{\dot{V}}{\pi haU}\right)^{\frac{1}{2}}\right] \tag{27}$$

in constrast to eq. (13). Either of the limits (11) or (13) is recovered by letting $\dot{V}/\pi haU$ increase without bound in eqs. (26) and (27). Eq. (25) is plotted in Fig. 7 showing the volume injected at breakthrough as a function of a dimensionless injection rate. The curve shows how, as injection rate increases, the breakthrough volume approaches the value given in eq. (13), that is, the value of the volume in Fig. 3 when concentration just starts to rise.

Again consider the recent example with a dimensionless injection rate of 1.0. From Fig. 7, the dimensionless volume at breakthrough is 0.19. The injected volume ($0.19*4\pi ha^2$) is thus 24 cc, less than the 42 cc earlier calculated for fast injection. Injecting 24 cc at 0.15 cc/min. takes 160 min.

Following breakthrough, the concentration of tracer arriving at the withdrawal hole will increase. As we did in the previous section, we must now examine the concentration increase during continuous injection. Generalizing eq. (14), we write now

$$f = \frac{2\,\mathrm{Im}(\Omega)h}{\dot{V}} + 1 \tag{28}$$

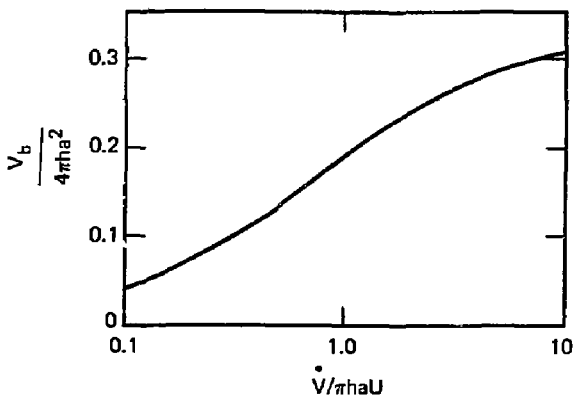

Figure 7. The volume injected, prior to breakthrough, increases as injection rate increases.

f is again equal to the arriving concentration ratio. Integrating velocity along this streamline yields the time at which this concentration is obtained. In dimensionless form, such integration produces

$$\frac{c}{c_o} = \frac{c}{c_o}\left(\frac{\dot{V}}{\pi h a U}, \frac{tU}{a}\right) \tag{29}$$

or, since V is $\dot{V}^*$ t,

$$\frac{c}{c_o} = \frac{c}{c_o}\left(\frac{\dot{V}}{\pi h a U}, \frac{V}{4\pi h a^2}\right) \tag{30}$$

Numerical integration in the complex plane was used to obtain results in this form. These results are shown in Fig. 8. Instead of the single curve of Fig. 3, we have a family of curves corresponding to different values of dimensionless flow rate. The infinite flow rate curve is the curve in Fig. 3. The intercept of each curve with the axis agrees with the breakthrough volume for Fig. 7.

With this result, we can continue with the example having a dimensionless injection rate of 1.0. We see again that the dimensionless volume at breakthrough is 0.19. Now we can also see the further evolution of the injection. If another equal volume is injected, the dimensionless volume is 0.38 and the concentration ratio is 0.78. At this point, 48 cc have been injected at 0.15 cc/min, taking 320 min.

The treatment of finite injections and retardation are as explained in the last section.

ACKNOWLEDGMENT

The author wishes to express his appreciation to Randy Stone and Don Helm for their very helpful comments and advice and to Dianne Oison for her excellent work in preparing this manuscript.

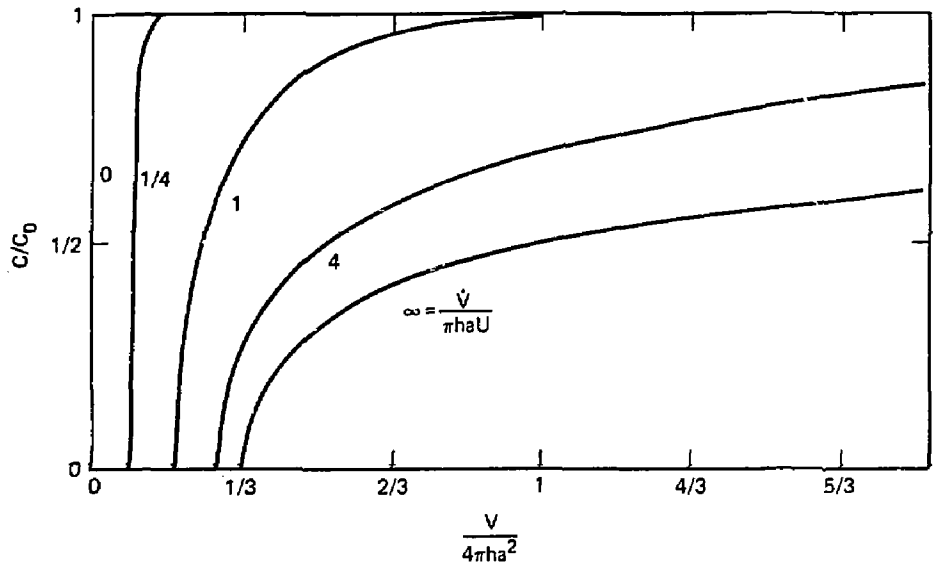

Figure 8. The concentration in the fluid arriving at the withdrawal borehole depends on the injection rate.

REFERENCES

1. D. B. Grove and W. A. Beetem, Porosity and Dispersion Constant Calculations for a Fractured Carbonate Aquifer Using the Two Well Tracer Method, Water Resources Research, 7, 128-134, 1971.

2. P. Moon and D. E. Spencer, Field Theory Handbook, Springer-Verlag, Berlin, 1971.

3. J. Bear, Dynamics of Fluids in Porous Media, American Elsevier, New York, 1972.

4. W. J. M. Rankine, On Plane Water Lines in Two Dimensions, Phil. Trans. Roy. Soc. London, 1864.

5. R. W. Nelson, Evaluating the Environmental Consequences of Groundwater Contamination Obtaining Location/Arrival Time and Location/Outflow Quantity Distributions for Steady Flow Systems, Water Resources Research, 14, 416-428, 1978.